Low-field magnetic properties as indication of disorder, frustration and cluster formation effects in $La_{1-x}Ca_xMn_{1-y}Fe_yO_3$

R. Laiho[a,*], K.G. Lisunov[a,b], E. Lähderanta[a,c], J. Salminen[a], V.S. Zakhvalinskii[a,b]

[a] *Wihuri Physical Laboratory, University of Turku, FIN-20014 Turku, Finland*
[b] *Institute of Applied Physics, Academiei Str., 5, MD-2028 Kishinev, Moldova*
[c] *Physics, University of Vaasa, P.O. Box 700, FIN-65101 Vaasa, Finland*

Abstract

Low-field ($B = 2-80$ G) DC magnetic susceptibility, χ, is investigated in ceramic $La_{1-x}Ca_xMn_{1-y}Fe_yO_3$ (LCMFO) samples with $x = 0.3$. When y is increased from 0 to 0.1 the ferromagnetic (FM) Curie temperature, T_C, decreases from 259 to 107 K, indicating growth of disorder by iron doping. A transformation of LCMFO from a weakly frustrated FM phase between $y \approx 0-0.05$ to a strongly frustrated mixed, FM and glassy, phase between $y \approx 0.07-0.10$ is revealed by measurements of magnetic irreversibility and long-time (up to $t = 10^5$ s) relaxation of thermoremanent magnetization. Critical behavior of $\chi(T)$ obeying the scaling law $\chi^{-1}(T)-\chi^{-1}(T_C) \sim (T/T_C-1)^{\gamma} \equiv \tau^{\gamma}$ is observed below $\tau_{cr} \sim 0.05-0.2$ with $\gamma = \gamma_1 \approx 1.4$ corresponding to a three-dimensional (3D) Heisenberg spin system. Above τ_{cr}, $\chi(T)$ can be fitted with the same scaling law as for $\tau < \tau_{cr}$, but with another value of $\gamma = \gamma_2 \approx 1.7$, which characterizes a 3D percolation system. The change of γ upon lowering the temperature can be explained by the formation of percolation clusters from an assembly of hole-rich nanoscale particles of the second FM phase embedded into the host LCMFO matrix at T well above T_C. The magnetic moments, radii, and concentration of these particles are determined.

1. Introduction

Interest to $La_{1-x}Ca_xMnO_3$ and related mixed-valence manganite perovskite compounds is connected to the "colossal" magnetoresistance (CMR) effect or huge decrease of the resistivity, ρ, in an external magnetic field, B, near the paramagnetic (PM) to ferromagnetic (FM) transition temperature, T_C [1]. The hole-doping of perovskites by substitution of a divalent alkaline element for La^{3+} introduces, besides Mn^{3+}, a fraction x of Mn^{4+} ions leading to FM Mn^{4+}–Mn^{3+} double exchange (DE) interactions competing with antiferromagnetic (AF) Mn^{3+}–Mn^{3+} superexchange

interactions [2]. In addition, extensive investigations have demonstrated that to understand the electronic and magnetic properties of CMR materials lattice effects and polaron formation should be taken into account [3], as well as magnetic frustration [4,5], charge ordering in half-doped manganites [6] and phase separation effects due to interplay between the charge, orbital and spin degrees of freedom [7,8].

Values of critical scaling exponents between predictions of the mean-field theory ($\beta = 0.5$, $\gamma = 1$) and the isotropic three-dimensional (3D) Heisenberg model ($\beta = 0.36$, $\gamma = 1.39$) [9] have been determined from modified Arrot plots of $La_{1-x}Sr_xCoO_3$ [10] and $La_{0.67}(Ba_xCa_{1-x})_{0.33}MnO_3$ [11], from measurements of microwave surface impedance of $La_{0.8}Sr_{0.2}MnO_3$ [12] and from magnetic susceptibility, χ, of $La_{0.95}Mg_{0.05}MnO_3$ [13]. On the other hand, investigations of χ in low fields [4,14] have revealed a group of ceramic LCMO samples with $x < x_b \approx 0.18$ and the hole concentration $c < c_b \approx 0.23$, exhibiting a clear second-order PM–FM transition with γ between 1 and 1.4, and another group with $x > x_b$ and $c > c_b$, having $\gamma = 1.64 \pm 0.06$ which are closer to 1.69 ± 0.05 and 1.70 ± 0.11 evaluated for a three-dimensional (3D) percolation system [15]. Furthermore, the giant $1/f$ noise observed in the conductivity of $La_{5/8-x}Pr_xCa_{3/8}MnO_3$ [16] and the critical behavior of the variable-range hopping conductivity in ceramic LCMO with $x = 0-0.15$ [17] are indicative of a percolation spin system in these compounds.

In efforts to expand the group of CMR materials attention has been paid to $La_{1-x}Ca_xMn_{1-y}Fe_yO_3$ (LCMFO) with similar ionic radii of Mn^{3+} and Fe^{3+} [18], causing minor lattice distortions by the substitution. At a low doping level direct replacement of Mn^{3+} by Fe^{3+} is expected [19], as well as introduction of additional AF interactions by Fe^{3+} ions [20] which do not support DE interactions in Fe^{3+}–Mn^{4+} pairs [21]. However, only a small amount of Fe, $y = 0.01-0.10$, is enough to influence strongly on transport and magnetic properties of LCMFO [18,21,22]. This is incompatible with damping only the DE interaction and suggests generation of an additional microscopic lattice disorder as a result of iron doping.

In this paper we report low-field magnetic susceptibility measurements in LCMFO. It is shown that such investigations may provide important microscopic information about the disorder and phase composition of the material.

2. Results and discussion

Samples of $La_{1-x}Ca_xMn_{1-y}Fe_y$ with $x = 0.3$ and $y = 0$, 0.01, 0.03, 0.05, 0.07, 0.09 and 0.10 (marked below as # 3–0, # 3–1, ..., # 3–10) were synthesized with standard ceramic procedure by heating stoichiometric mixtures of La_2O_3, $CaCO_3$ Mn_2O_3 and Fe_2O_3 in air, with intermittent grindings. According to X-ray diffraction measurements all the samples have the same undistorted cubic structure (space group Pm3m) as the undoped material [4,17]. The temperature dependence of the magnetization, $M(T)$, was measured with an RF-SQUID magnetometer after cooling the samples from the room temperature down to 5 K in zero field (ZFC) or in DC field of $B = 2$, 20 or 80 G (FC). For investigations of the time decay of the thermoremanent magnetization (TRM) the sample was first cooled in the field of 5 G from the room temperature down to the measuring temperature, T_m. After a wait time, t_W, the field was abruptly reduced to zero and the decay of TRM was recorded over a time period up to $t \sim 10^5$ s.

As shown in Fig. 1, the susceptibilities $\chi_{ZFC}(T)$ and $\chi_{FC}(T)$ of samples # 3–0, # 3–1, # 3–3 and # 3–5 exhibit a sharp FM transition at T_C which moves to a lower temperature when y is increased. Additionally, magnetic irreversibility or deviation of $\chi_{ZFC}(T)$ from $\chi_{FC}(T)$ is observed just below the transition. At $T < T_C$ the temperature dependencies of $\chi_{ZFC}(T)$ and $\chi_{FC}(T)$ are weak and close to linear, while their difference is decreased when B is increased. Generally, the shapes and the values of $\chi_{ZFC}(T)$ and $\chi_{FC}(T)$ shown in Fig. 1 resemble closely those of undoped LCMO with x between 0.2–0.4 and $c \approx 0.24-0.43$ [4,17] and are typical for a disordered ferromagnet. On the other hand, in samples # 3–7, # 3–9 and # 3–10 the behavior of $\chi(T)$ is quite different (see Fig. 2). The temperature dependence of χ_{ZFC} below T_C is stronger, and has below the onset of the irreversibility a clear

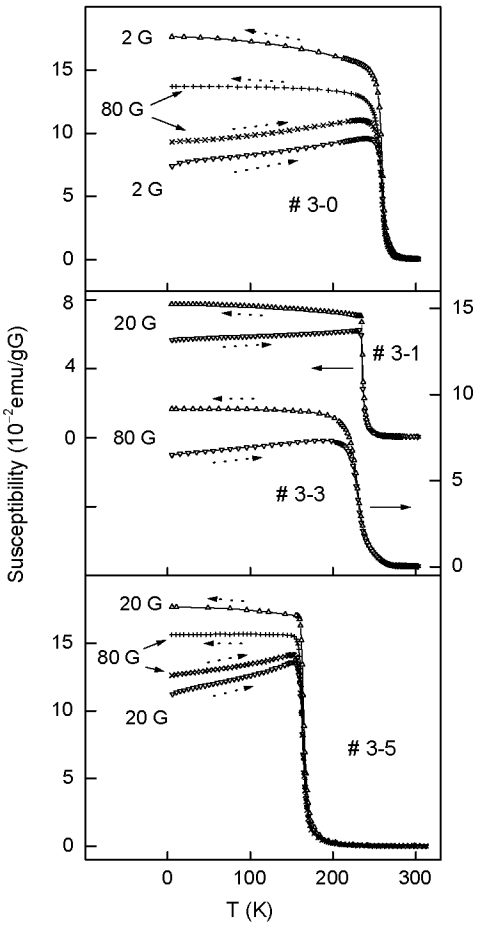

Fig. 1. Temperature dependence of the susceptibility of samples # 3–0, # 3–1, # 3–3 and # 3–5.The dotted arrows mark the ZFC and the FC branches.

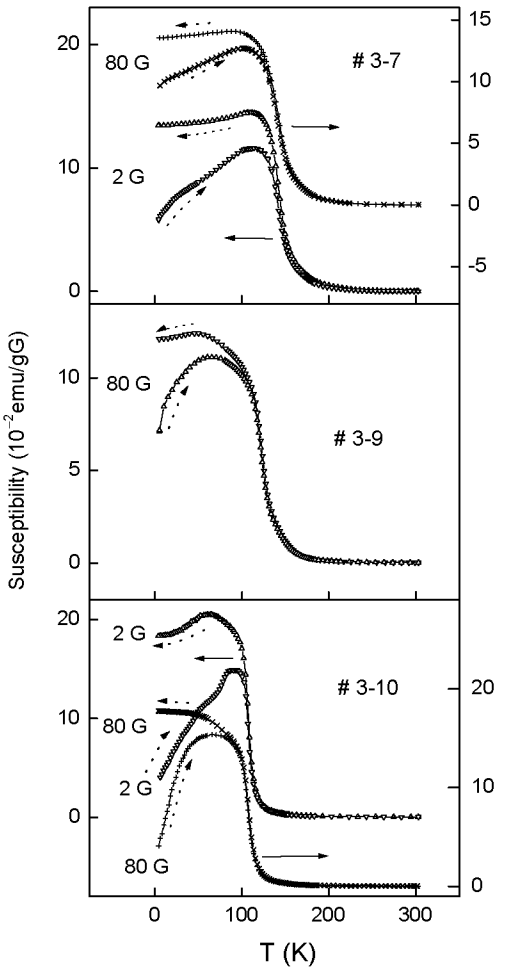

Fig. 2. Temperature dependence of the susceptibility of samples # 3–7, # 3–9 and # 3–10. The dotted arrows mark the ZFC and the FC branches.

maximum, which becomes more rounded and is shifted to lower temperatures when B is increased. Such features are pertinent to a spin-glass or a cluster-glass phase.

As can be seen in Fig. 3 (upper panel) the relaxation of TRM at low temperatures, observed over a time scale up to 10^5 s, increases strongly with growing y (between $T_m \sim 5-25$ K the relaxation of TRM exhibits only a weak sensitivity to T_m or t_W). In addition, the time dependence of TRM in # 3–3 and 3–5 is much weaker than that observed in # 3–7 and 3–10, respectively. For the last pair of samples the relaxation of TRM is found to be strong enough to evaluate the corresponding relaxation rates, $S = -d$ TRM $(t)/d \log t$, which are plotted for # 3–7 at $t_W \approx 3700$ s and for # 3–10 at $t_W = 3700$ and 1900 s (see the lower panel of Fig. 3). Each curve of $S(t)$ displays a clear maximum near the wait time which is shown by the vertical dotted line.

Aging effects closely similar to those in Fig. 3 are often observed in a glassy phase or a FM phase of a re-entrant spin-glass [23], indicating the specific non-equilibrium character of frustrated magnetic systems. The long-time relaxation phenomena in our LCMFO samples (Fig. 3) exhibit a

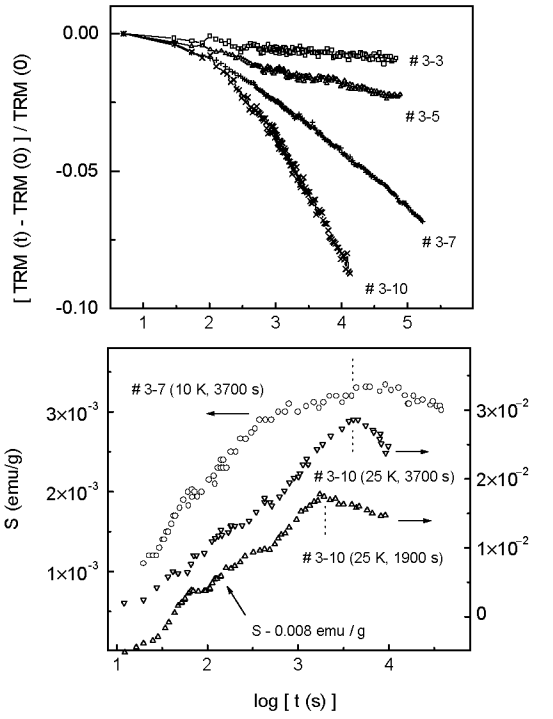

Fig. 3. Upper panel: the relaxation of the low-temperature TRM for samples # 3–3, # 3–5, # 3–7 and # 3–10 (T_m between 5 and 25 K, τ_W between 10^3 and 10^4 s). Lower panel: the relaxation rate vs. time for samples # 3–7 and # 3–10. In parenthesis are shown the values of T_m and τ_W. For convenience one of the curves is shifted for 0.008 emu/g along the S-axis.

clear correlation with the magnetic irreversibility measurements (cf. Figs. 1 and 2), giving evidence for the transformation of LCMFO from a weakly frustrated FM phase to a strongly frustrated mixed (FM and glassy) phase with increasing y. In turn, this reflects the growth of disorder introduced by doping with Fe. If we assume that Fe^{3+} does not take part in the DE interactions [21], the observed increase of the magnetic irreversibility and the long-time relaxation with growing y can be explained by increasing frustration due to random breaking of the DE interaction by Fe^{3+} ions in the Fe^{3+}–Mn^{4+} pairs. This agrees qualitatively with the de Almeida model [24], which predicts a frustrated magnetic ground state for systems containing lattice disorder and competing SE–DE interactions.

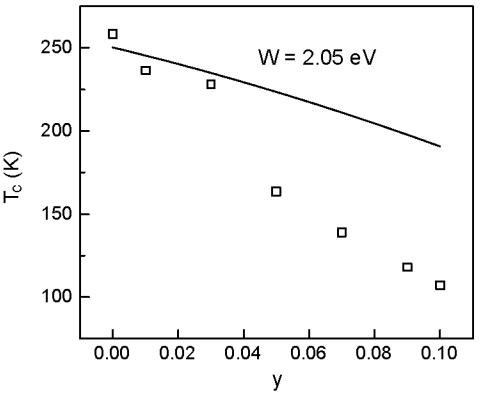

Fig. 4. The dependence of T_C on y. The solid line is calculated from Eq. (1) as described in the text.

Another manifestation of disorder is the strong decrease of T_C when y is increased, as can be seen from Fig. 4. To discuss the dependence of T_C on y, we apply the model of Varma [25], which treats the PM–FM transition in La manganites by considering the localization of charge carriers by magnetic disorder and Coulomb interaction. The carriers are localized below the mobility threshold within a band with the width W and rectangular shape of the density of states. According to this model, T_C is given by the equation

$$kT_C \approx 0.05 W_c(1-c). \quad (1)$$

Using two series of undoped $La_{1-x}Ca_xMnO_3$ samples a good agreement with the experimental data of $T_C(x)$ is obtained, yielding $W = 1.90 \pm 0.05$ [4] and 1.88 ± 0.06 eV [17]. In LCMFO, assuming a direct replacement of Mn^{3+} by Fe^{3+} [20] and that Fe^{3+} ions do not support the DE interaction in Fe^{3+}–Mn^{4+} pairs [21], we would have $c \approx x - y$. Then from Eq. (1) it follows that T_C should be a decreasing function of y, in a qualitative agreement with the observed dependence of T_C on the Fe concentration. However, as evident from Fig. 4, the plot of $T_C(y)$ evaluated from Eq. (1) with $W = 2.05$, which is close to that in undoped LCMO, is in line with the experimental data for $y \leqslant 0.03$, but exceeds considerably those for $y \geqslant 0.05$. Therefore, damping of the DE interaction by Fe^{3+} ions is insufficient to explain the decrease of T_C when y is increased.

Despite the similarity of the radii of Mn^{3+} and Fe^{3+} ions, doping with Fe is expected to increase disorder by introducing additional microscopic lattice defects, which favor the localization of charge carriers by decreasing the localization radius. This should lead to narrowing of the bandwidth W of the localized states when y is increased, bringing an additional contribution to diminution of T_C according to Eq. (1). It is worth noting, that a strong decrease of the localization radius of charge carriers with increasing Fe concentration has been concluded from analysis of the temperature dependence of the resistivity in LCMFO [22,26], assuming the Mott [27] or even more consistent Shklovskii–Efros [28] mechanisms of variable-range hopping conductivity.

For the next, we discuss the behavior of $\chi(T)$ above the FM–PM transition in LCMFO. We restrict ourselves to the samples with $y \geqslant 0.05$ having T_C well below the room temperature (Fig. 4). This allows us to investigate a sufficiently wide temperature interval to understand the magnetic behavior of the samples above T_C in detail.

As $T \to T_C$ from the PM side, $\chi(T)$ is expected to follow the scaling law, $\chi(T) \sim (T/T_C - 1)^{-\gamma}$, connected to enhancement of short-range FM fluctuations when approaching the PM–FM transition [9]. For the analysis of the experimental data it is convenient to write

$$\chi^{-1} - \chi_C^{-1} \sim \tau^{\gamma} \tag{2}$$

with $\chi_C = \chi(T_C)$ and $\tau = T/T_C - 1$. For temperatures not sufficiently close to T_C, Eq. (2) must be modified by adding a correction-to-scaling term [29],

$$\chi^{-1} - \chi_C^{-1} \sim \tau^{\gamma}(1 + C\tau^{p}), \tag{3}$$

where C is the correction-to-scaling amplitude and p is the correction-to-scaling exponent. The plots of $\ln(\chi^{-1} - \chi_C^{-1})$ vs. $\ln \tau$ for $\chi_{ZFC}(T)$ and $\chi_{FC}(T)$ measured in different fields for samples # 3–5, 3–7 and 3–10 are shown in Fig. 5 (those of # 3–9 are similar to # 3–10). For all samples, independent of the cooling conditions (ZFC or FC) and applied field, these plots contain below a certain τ_{cr} a linear part with the same slope γ_1. The values of γ_1 and τ_{cr} are collected in Table 1. They are close to $\gamma =$ 1.39–1.43 in $La_{1-x}Sr_xCoO_3$ [10], $\gamma = 1.39 \pm 0.05$ in $La_{0.95}Mg_{0.05}MnO_3$ [13] and $\gamma = 1.45$ in a LCMO single crystal with $x = 0.2$ [30], corresponding to

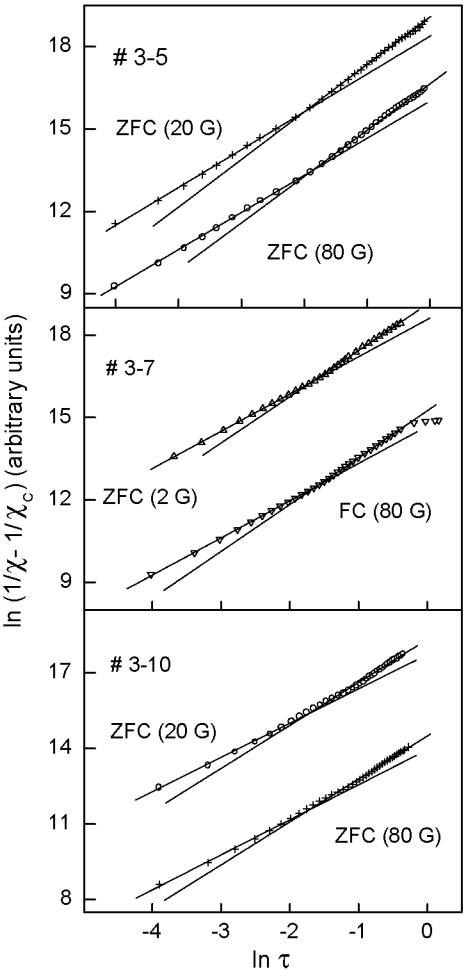

Fig. 5. The plots of $\ln(1/\chi - 1/\chi_c)$ vs. $\ln \tau$ for samples # 3–5, # 3–7 and # 3–10. The solid lines represent linear fits.

Table 1
Values of the critical exponents γ_1 and γ_2 and τ_{cr} for the LCMFO samples

Sample no.	γ_1	γ_2	τ_{cr}
# 3–5	1.36±0.02	1.72±0.03	0.13
# 3–7	1.37±0.01	1.71±0.03	0.21
# 3–9	1.41±0.02	1.70±0.03	0.20
# 3–10	1.40±0.03	1.71±0.03	0.17

the 3D Heisenberg spin system [9]. In Fig. 6 are shown fits of $\ln(\chi^{-1}-\chi_C^{-1})$ vs. $\ln\tau$ with Eq. (3), treating C and p as adjustable parameters and γ equal to γ_1. The values of $C = 1.6\pm0.4$, 1.2 ± 0.2, 1.1 ± 0.3 and $p = 1.2\pm0.2$, 1.7 ± 0.1 and 1.0 ± 0.3 for samples # 3–5, # 3–7 and # 3–10, respectively, exhibit large scattering between the samples and from one curve to another measured in different fields and cooling regimes even for one and the same sample. Additionally, the values of p are found to be $\sim$2–3 times higher than that predicted for the 3D Heisenberg system, $p = 0.550\pm0.005$ [9]. On the other hand, the values of $\beta = 0.38\pm0.01$ and $p = 0.4\pm0.1$, obtained in neutron diffraction measurements for LCMFO with $y = 0.01$ over a broad interval of T between 2 K and $T_C \approx 260$ K [20], agree well with the 3D Heisenberg universality class predictions [9]. Hence, despite the rather good fit in Fig. 6, Eq. (3) fails to describe correctly the temperature dependence of the susceptibility of # 3–5, 3–7 and 3–10 beyond the asymptotic interval of $T \to T_C$.

We attribute this discrepancy to the phase separation effect being responsible for creation of small hole-rich FM particles in the PM or AF host matrix at T well above T_C [31,32]. When T is decreased, both the radius r and the volume fraction, $\eta(r)$, of these particles are increased, joining them into strongly correlated FM clusters. When the correlation length $\lambda \approx R\tau^{-\nu}$ [28], where $R \approx 2(4\pi n/3)^{-1/3}$ is the mean distance between the particles, n is their concentration and $\nu \approx 1$ is the critical exponent of λ, becomes much longer than the lattice parameter a, a scaling behavior of $\chi(T)$ similar to Eq. (2) but with another value of the critical exponent γ can be expected due to the percolation character of these clusters [28]. As can be seen from Fig. 5, above τ_{cr} the plots of $\ln(\chi^{-1}-\chi_C^{-1})$ vs. $\ln\tau$ in # 3–5, 3–7 and 3–10 can be characterized by a second linear part. The values of the slopes of the second linear parts for $\tau > \tau_{cr}$, γ_2, are quite close for different samples (see Table 1) and characterize a 3D percolation spin system [15].

The parameters of the FM particles at high temperatures can be estimated by treating them roughly as an assembly of independent weakly correlated carriers of moments. Assuming that

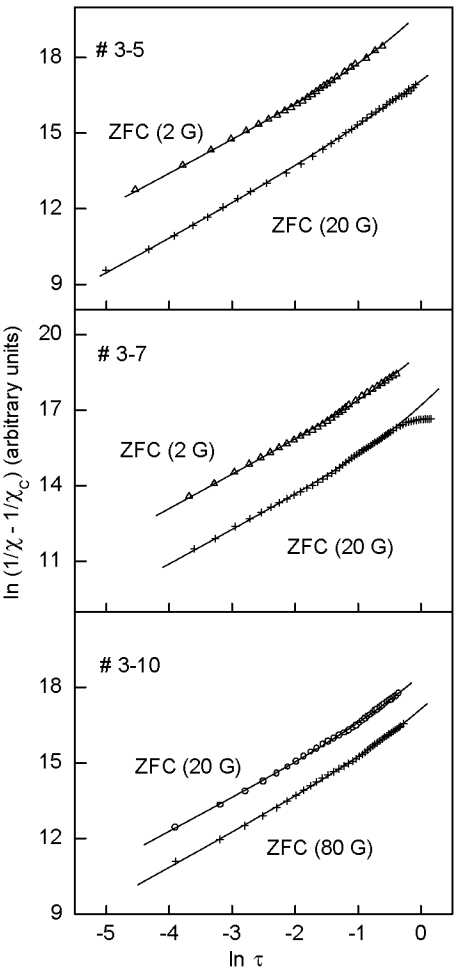

Fig. 6. Analysis of the temperature dependence of the susceptibility in # 3–5, # 3–7 and # 3–10 with the correction-to-scaling law. The solid lines are calculated with Eq. (3) as described in the text.

they have at $T^* = 300$ K a predominant contribution to $M(T^*)$, we can express the magnetization approximately as $M(T^*) \approx \mu n L(\mu B/kT^*)$, where μ is the moment of the FM particle and $L(\xi)$ is the Langevin function, which for $\xi \ll 1$ gives $\chi(T^*) \approx \mu^2 n/(3kT^*)$. The volume fraction of the second phase satisfies the equation $\eta \approx \mu n/M_s$, where M_s is the saturation magnetization which has been determined for LCMFO in [18,20,21]. From the above expressions we obtain

$$\mu \approx 3kT^*\chi(T^*)/M_s\eta \tag{4}$$

and

$$n \approx \eta^2 M_s^2/[3kT^*\chi(T^*)]. \quad (5)$$

If r_c is the critical value of r corresponding to the percolation threshold, τ can be presented in the form $\tau = r_c/r - 1$. Then, taking into account that the volume fraction satisfies the equation [28]

$$\eta = 1 - \exp(-4\pi n r^3/3) \quad (6)$$

and that $\eta_c = \eta(r_c) = 0.29$ [28], we obtain

$$\eta = 1 - (1 - \eta_c)^{1/(1+\tau)^3}. \quad (7)$$

with Eqs. (4)–(7) for y between 0.05 and 0.10 we estimate $r \approx 2$–3 nm, $\mu \approx (1-3) \times 10^3\,\mu_B$, $\eta \approx 0.02-0.05$ and $L/a \approx 15-20$, using the data of M_s from [18,20,21] and the values of χ (300 K) $\approx (2.8$–$2.0) \times 10^{-4}$ emu/g G for samples # 3–5 to # 3–10, respectively. The results obtained for different samples are similar, the values of r and μ correspond to the nanoscale FM particles, and those of L/a are large enough to provide the onset of the percolation behavior even at or near the room temperature, being consistent with the corresponding onset of the second slope in Fig. 5. The estimation of n gives $\sim 10^{17}$–10^{18} cm^{-3}, suggesting a stronger dependence of n on y than for the other parameters. However, the method above does not permit to obtain more accurate data to support this conjecture.

A similar non-universal critical behavior of $\chi(T)$, characterized by the 3D Heisenberg value of $\gamma \approx 1.37$–1.38 at $\tau < \tau_{cr}$ and by the 2D percolation value of $\gamma \approx 2.4$ [28] at $\tau > \tau_{cr}$, has been observed recently in $La_{0.7}Ca_{0.3}MnO_3$ thin films and explained by the phase separation effect, too [33]. The estimations above yield values of n lying between $n = 2.1 \times 10^{19}$ cm^{-3}, as found for bulk $La_{1-x}Ca_xMnO_3$ with $x = 0.05$ and 0.08 in neutron scattering experiments [32], and $n \approx (1-4) \times 10^{16}$ cm^{-3}, as estimated in Ref. [33]. On the other hand, the values of r found above are similar to $r \approx 5$ nm obtained by Mössbauer investigations at T just below T_C in $La_{0.8}Ca_{0.2}MnO_3$ [31]. This gives additional support to the existence of the percolation subsystem built from FM particles of the second (hole-rich) phase, which determines the behavior of the susceptibility in LCMFO for $\tau > \tau_{cr}$.

3. Conclusions

Low-field magnetic properties of LCMFO samples with $x = 0.3$ and $y = 0-0.1$ are investigated. For $T < T_C$ increasing magnetic frustration leads to enhancement of the magnetic irreversibility and the aging effects when y is increased. A transformation of LCMFO from a weakly frustrated FM phase between $y \approx 0-0.05$ to a strongly frustrated mixed FM and glassy phase between $y \approx 0.07-0.10$ is observed. At the same time, T_C exhibits a strong dependence on Fe concentration, decreasing when y is increased. Both the rise of the magnetic frustration and enhancement of the related phenomena and the shift of the PM–FM transition to lower temperatures can be interpreted as a result of increasing lattice disorder introduced by doping with Fe.

For $T > T_C$ an unusual non-universal critical behavior of $\chi(T)$, characterized by different values of the critical exponent γ within two temperature intervals, is observed. Close to T_C, the value of $\gamma \approx 1.4$ corresponds to a conventional scaling behavior due to enhancement of the short-range FM fluctuations in a 3D Heisenberg spin system. Outside the asymptotic interval of $T \to T_C$ and up to the room temperature, the value of $\gamma \approx 1.7$ indicates formation of percolation clusters by growing of the volume and the moments of the FM particles of the second phase when T is decreased. The radius, the magnetic moment and the concentration of the FM particles are estimated in a reasonable agreement with the literature data, including those obtained from microscopic investigations of $La_{1-x}Ca_xMnO_3$.

Acknowledgements

This work was supported by the Wihuri Foundation, Finland, and by INTAS (Project No. INTAS 00-00728).

References

[1] R. von Helmolt, J. Wecker, B. Holzapfel, L. Schulz, K. Sammer, Phys. Rev. Lett. 71 (1993) 2331;

P. Schiffer, A.P. Ramirez, W. Bao, S.-W. Cheong, Phys. Rev. Lett. 75 (1995) 3336.
[2] C. Zener, Phys. Rev. 82 (1951) 403;
P.-G. de Gennes, Phys. Rev. 118 (1960) 141.
[3] M. Jaime, P. Lin, S.H. Chun, M.B. Salamon, P. Dorsey, M. Rubinstein, Phys. Rev. B 60 (1999) 1028;
T.T. Palstra, A.P. Ramirez, S.-W. Cheong, B.R. Zegarski, P. Schiffer, J. Zaanen, Phys. Rev. B 56 (1997) 5104.
[4] R. Laiho, K.G. Lisunov, E. Lähderanta, P.A. Petrenko, J. Salminen, V.N. Stamov, V.S. Zakhvalinskii, J. Phys.: Condens. Matter 12 (2000) 5751.
[5] R. Laiho, E. Lähderanta, J. Salminen, K.G. Lisunov, V.S. Zakhvalinskii, Phys. Rev. B 63 (2001) 094405.
[6] C.H. Chen, S.-W. Cheong, Phys. Rev. Lett. 76 (1996) 4042.
[7] S. Yunoki, A. Moreo, E. Dagotto, Phys. Rev. Lett. 81 (1998) 5612;
S. Okamoto, S. Ishihara, S. Makaeva, Phys. Rev. B 61 (2000) 451.
[8] G. Papavassiliou, M. Fardis, M. Belesi, T.G. Maris, G. Kallias, M. Pissas, D. Niarchos, C. Dimitropulos, J. Dolinsek, Phys. Rev. Lett. 84 (2000) 761.
[9] J.C. Le Guillou, J. Zinn-Justin, Phys. Rev. Lett. 39 (1977) 95.
[10] J. Mira, J. Rivas, M. Vazques, J.M. Garcia-Beneyetz, J. Arcas, R.D. Sanchez, M.A. Senaris-Rodriguez, Phys. Rev. B 59 (1999) 123.
[11] N. Moutis, I. Panagiotopulos, M. Pissas, D. Niarchos, Phys. Rev. B 59 (1999) 1129.
[12] A. Schwartz, M. Scheffler, S.M. Anlage, Phys. Rev. B 61 (2000) R870.
[13] J.H. Zhao, T. Song, H.P. Kunkel, X.Z. Zhou, R.M. Roshko, G. Williams, J. Phys.: Condens. Matter 12 (2000) 6903.
[14] R. Laiho, K.G. Lisunov, E. Lähderanta, P.A. Petrenko, J. Salminen, V.N. Stamov, V.S. Zakhvalinskii, J. Phys.: Condens. Matter 12 (2000) 5751.
[15] M.F. Sykes, J.W. Essam, Phys. Rev. 133 (1964) 310;
A.G. Dunn, J.W. Essam, D.S. Ritchie, J. Phys. C 8 (1975) 4219.
[16] V. Podzorov, M. Uehara, M.E. Gershenson, T.Y. Koo, S.-W. Cheong, Phys. Rev. B 61 (2000) R3784.
[17] R. Laiho, K.G. Lisunov, E. Lähderanta, V.N. Stamov, V.S. Zakhvalinskii, J. Phys.: Condens. Matter 13 (2001) 1233.
[18] K.H. Ahn, X.W. Wu, K. Liu, C.L. Chien, Phys. Rev. B 54 (1996) 15299.
[19] G.H. Jonker, Physica 20 (1954) 1118.
[20] A. Simopoulos, M. Pissas, G. Kallias, E. Devlin, N. Moutis, I. Panagiotopoulos, D. Niarchos, C. Christides, R. Sonntag, Phys. Rev. B 59 (1999) 1263.
[21] K.H. Ahn, X.W. Wu, K. Liu, C.L. Chien, J. Appl. Phys. 81 (1997) 5505.
[22] S.K. Hasanain, M. Nadeem, W.H. Shah, M.J. Akhtar, M.M. Hasan, J. Phys.: Condens. Matter 12 (2000) 9007.
[23] K. Jonason, J. Mattson, P. Nordblad, Phys. Rev. B 53 (1996) 6507.
[24] J.R.L. de Almeida, J. Phys.: Condens. Matter 11 (1999) L223.
[25] C.M. Varma, Phys. Rev. B 54 (1996) 7328.
[26] R. Laiho, E. Lähderanta, J. Salminen, K.G. Lisunov, V.S. Zakhvalinskii, M.O. Safontchik, M.A. Shakhov, M.L. Shubnikov, J. Appl. Phys. 91 (2002) 7400.
[27] N.F. Mott, Metal-Insulator Transitions, Taylor & Francis, London, 1990.
[28] B.I. Shklovskii, A.L. Efros, Electronic Properties of Doped Semiconductors, Springer, Berlin, 1984 (Chapter 5).
[29] F.J. Wegner, Phys. Rev. B 5 (1972) 4529.
[30] C.S. Hong, W.S. Kim, N.H. Hur, Phys. Rev. B 63 (2001) 092504.
[31] V. Chechersky, A. Nath, I. Isaac, J.P. Franck, K. Ghosh, H. Ju, R.L. Greene, Phys. Rev. B 59 (1999) 497.
[32] M. Hennion, F. Moussa, G. Biotteau, J. Rodriguez-Carvajal, L. Piusard, A. Revcolevschi, Phys. Rev. Lett. 81 (1998) 1957.
[33] H. Huhtinen, R. Laiho, E. Lähderanta, J. Salminen, K.G. Lisunov, V.S. Zakhvalinskii, J. Appl. Phys. 91 (2002) 7944.